Improvement of the Efficiency in Lunar Surface Excavation with Vibration

Takaaki Inada, Takaaki Yokoyama and Kazuyoshi Tateyama

September 23, 2021

IMPROVEMENT OF THE EFFICIENCY IN LUNAR SURFACE EXCAVATION WITH VIBRATION

Takaaki Inada[a] , Takaaki Yokoyama[a] , Kazuyoshi Tateyama[a]

[a] *Depertment of Science and Engineering, Ritsumeikan University, JAPAN*
rv0058hh@ed.ritsumei.ac.jp, t-yoko@fc.ritsumei.ac.jp, tateyama@se.ritsumei.ac.jp

Abstract

Backhoe may become unstable in excavation work on lunar surface because it is difficult to obtain excavation reaction force due to compacted regolith ground and low gravity on the moon. We suggest vibration excavation for an effective technique on the moon. The goal of this study is to grasp the relation between inter friction angle and vibration as a basic research to show that the effect of vibration on the excavation is an effective technique on the moon. As a result of the experiment, it was confirmed that the internal friction angle tends to decrease with increasing vibration.

Keywords: Lunar surface, Vibration excavation, Internal friction angle, Vibration energy, Excavation reaction force

1. Introduction

For these days, reusable rockets such as SpaceX have been attracting attention. The reusable rocket will lead to lower costs for launching rockets and the challenge to explore space will be increase. Therefore, it is expected to promote space exploration. The moon is attracting attention as a base for space exploration. For lunar exploration, it is essential to establish the technology of excavation of lunar soil for scientific exploration on the moon and construction of a base lunar surface. However, on the lunar surface, the gravity is 1/6, and the regolith, the sand of lunar surface, is compacted hardly. The necessary excavation reaction force cannot be obtained, and the construction equipment cannot excavate deeply so efficient excavation is difficult. On the earth, a method of increasing the weight of construction equipment is adopted in order to obtain the excavation reaction force, but in the case of the moon, the weight that can be transported is limited, because of technically and cost-effectively viewpoints. Therefore, an efficient excavation method using light construction equipment that can be transported to the lunar surface is required. We focus on the phenomenon that the internal friction angle that causes shear resistance is reduced in an environment where granules such as sand were vibrated, and propose an excavation method using the vibrated blade at the tip of the excavation bucket (Hata, 1968).

In this paper, as a basic study, the relationship between the vibration and the angle of internal friction, which indicates the strength of the soil, and the effect of the frequency and amplitude of vibration on the internal friction angle depending on the particle size are clarified.

2. Experimental set up

2.1 Experimental device

The purpose of this study was to determine the relationship between the angle of internal friction and vibration, as well as the effect of vibration on the angle of internal friction depending on the particle size. Using the apparatus shown in Fig. 1, experiments that a vibrating aluminum plate (in the paper referred to as vibrating blade) was sunk into the simulated lunar ground was conducted. The device shown in Fig. 1, the vibrating blade is fixed at pipe by the clamp and can be dropped by manually loosening the clamp. After losing the clamp the vibrating blade can be moved freely in vertical direction.

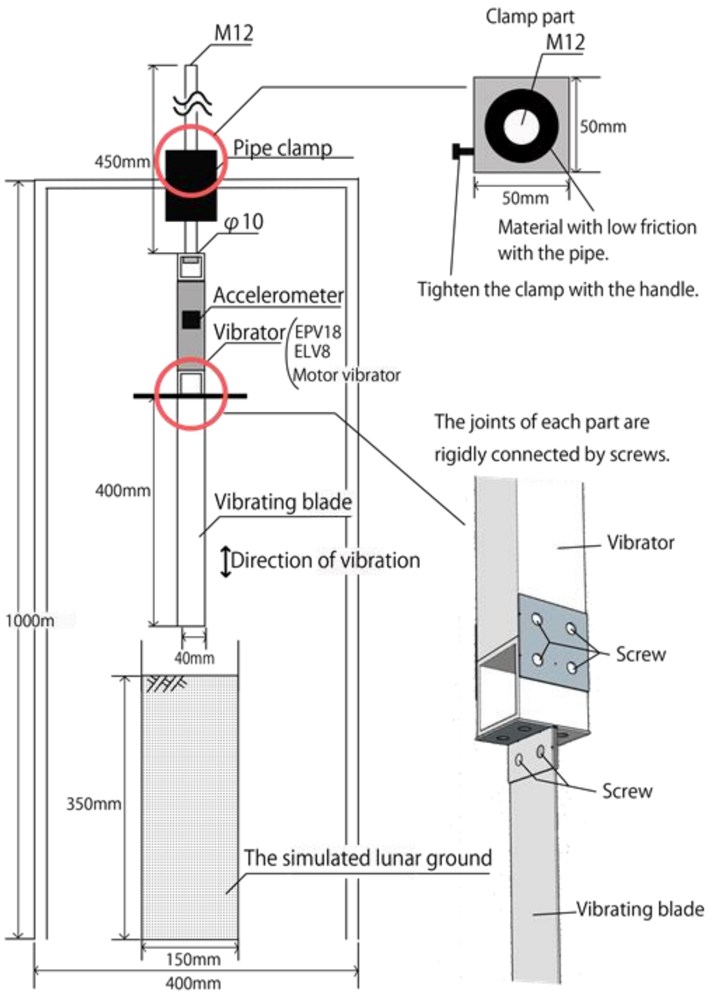

__Fig. 1.__ Experimental equipment used in self-weight loading experiment

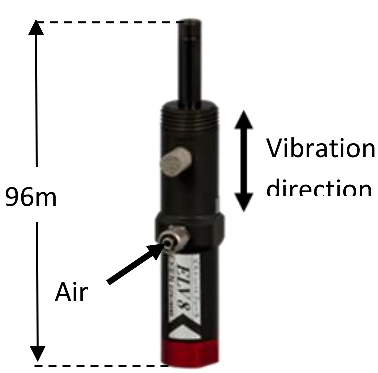

(a) ELV8 (Air vibrator)

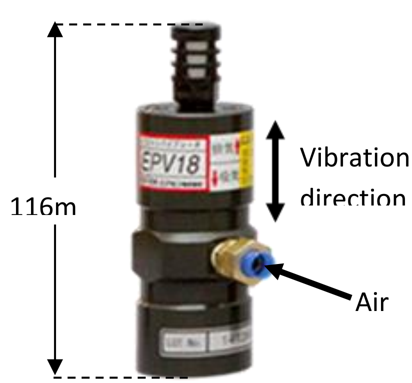

(b) EPV18 (Air vibrator)

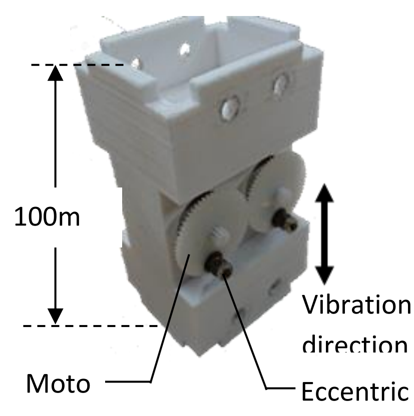

(c) Motor vibrator

__Fig. 2.__ Air vibrators used in self-weight loading experiment

Table 1. The specifications of the three types of vibrators

	Frequent [Hz]	Amplitude [m]	Size
ELV8 (Air vibrator)	About 60	0.001 ~ 0.009	H 96mm × φ 8mm
EPV18 (Air vibrator)	90 ~ 140	0.001 ~ 0.007	H 116mm × φ 38mm
Motor vibrator	50 ~ 60	0.0009 ~ 0.002	H 100mm × W 60mm × L 50mm

The vibrating blade was designed with a length of 400 mm and a width of 40 mm. Figure-2 shows the vibrator used in these experiments, and Table-1 shows the specifications of the three types of vibrators shown in Fig. 2. The Fig. 2 shows the air vibrators manufactured by Exen and handmade motor vibrator that attached eccentric weight to two motors and operated by a DC power supply. Frequency and amplitude depend on the air pressure and voltage used, so they cannot be adjusted to any value. Since these vibrators move only in the vertical direction, so horizontal vibration is not considered in these experiments.

2.2 *Experimental method*

The experiment was carried out according to the experimental procedure as follows.

(1) The tip of the vibration blade was set on the surface of the sand.
(2) The settlement was set to 0 at the location of step (1).
(3) The clamp was loosened and the vibrating blade was sunk with the self-weight of the device.
(4) The settlement was measured after finishing sinking in the step (3) (This is initial settlement).
(5) The vibrator and accelerometer was operated at the same time, the vibrating blade was sunk again.
(6) The accelerometer was stopped 3 seconds after step (5) to properly evaluate the effects of vibration on the ground.
(7) The settlement was measured when the settlement due to vibration is completed (This is final settlement).

In this experiment, we acquired three data: frequency and amplitude, settlement of vibration blade. In this experiment, the air pressure and voltage were varied, the frequency was determined from the results of Fourier analysis of the waveform measured by the accelerometer which attached on the vibration blade. The amplitude of the vibration was calculated by double integral of the acceleration obtained by the accelerometer. When step (5) was completed, it was considered that the weight of the vibrating blade and the friction force from the ground were balanced. It is assumed that a triangular distribution of the soil pressure is applied to both sides of the vibrating blade based on Rankine's theory of earth pressure. This soil pressure can be calculated from the weight of the vibrating blade and the amount of subsidence that were balanced with the friction force from the ground. Equation (1) is Rankine's earth pressure equation multiplied by the coefficient of friction μ between the soil and the blade. The internal friction angle ϕ is calculated from the earth pressure coefficient k included in Eq (1).

$$F = k\gamma BH^2 \cdot \mu \quad (1)$$

In this experiment, F is the self-weight of the vibrating blade includes the pipe and other experimental devices, B is the vibrating blade width, H is the amount of subsidence of the vibrating blade, and γ is the unit volume weight of soil. The earth pressure coefficient is $k = \tan^2\left(\frac{\pi}{4} + \frac{\phi}{2}\right)$, and the unit volume weight of soil and friction coefficient are measured by the following method prior to this experiment.

The coefficient of friction is calculated by sliding the vibrating blade on the sand ground as shown in Fig. 3 by dividing the pulling force of the spring weigher by the vertical load acting on the vibrating blade. In general, it is said that the friction coefficient decreases with the vibration (Hata, 1968).

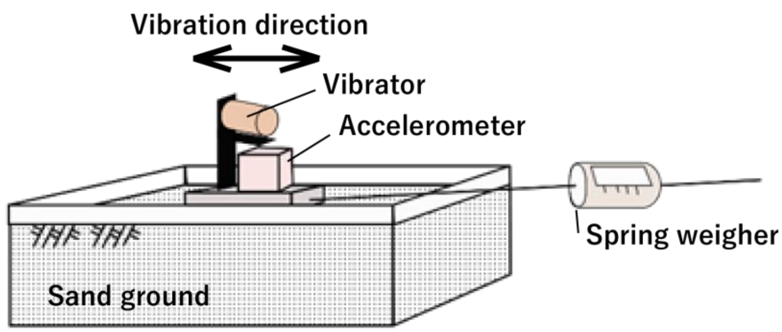

Fig. 3. *Simple measurement of coefficient of friction*

Since the direction of vibration was considered only for the vertical direction as described main experiment, only the horizontal direction is considered in this measurement. In this experiment, Nas Fine Sand (hereafter referred to as BFNS) and Toyoura sand (fine sand) were used for comparison. Silica sand No. 3, No. 5 and No. 8 were also used to check the effect of different particle size on the frequency and amplitude on the internal friction angle. BFNS is a fine-grained slag generated as a byproduct during the smelting of ferronickel, a raw material for stainless steel. Figure 4 (a) shows the results of this measurement for BFNS and Toyoura sand, and Fig. 4-(b) for Silica sand No. 3, No. 5, and No. 8. For the fitted curves shown in Fig. 4, the result of $R^2 > 0.7$, which is generally said to show high correlation, is adopted. Figure 4 (a) shows that the friction coefficient of the BFNS is larger than that of the Toyoura sand when measured without vibration (vibration acceleration of 0 m/s^2). It can also be seen that the rate of decrease in the coefficient of friction of BFNS is greater than that of Toyoura sand when subjected to vibration. It can also be confirmed from Fig. 4-(b) that the smaller the particle size, the larger the friction coefficient.

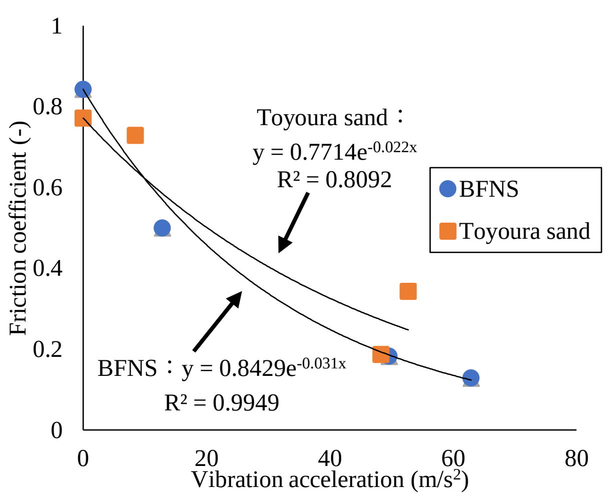

(a) Toyoura sand and BFNS

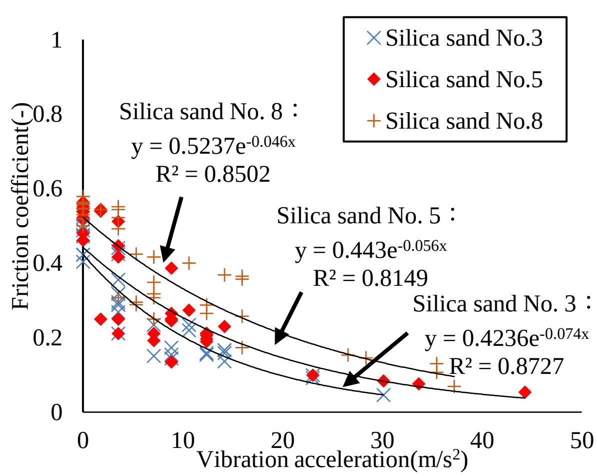

(b) Silica sand No.3, No.5, No.8

Fig. 4. *Results of a simple measurement of the coefficient of friction using the vibrating blade*

2.3 Ground conditions

Lunar regolith is a deposit of crushed meteorites and dust from the impact of the moon. Therefore, the physical properties of BFNS and lunar regolith are considered to be similar due to their formation process. Figure 5 shows the particle size distribution curves of the sand, excluding the regolith, used in this experiment. Figure 5-(a) shows the particle size distribution curves for BFNS and Toyoura sand, Fig. 5-(b) shows the results of particle size distribution curves for Silica sand No. 3, Silica sand No. 5, and Silica sand No. 8, where D_{50} is the particle size corresponding to 50% of the passing mass percentage. Figure 6 shows a micrograph of the sand sample used in this experiment. Figure 6-(a) shows Toyoura sand, (b) shows BFNS, (c) shows regolith simulant at 2000x magnification, respectively. In Fig. 6, there is a difference in images due to the difference in particle size. Fig. 6-(a) shows the surface of a sand particle, Fig. 6-(b) and Fig. 6-(c) show the entire sand particle.

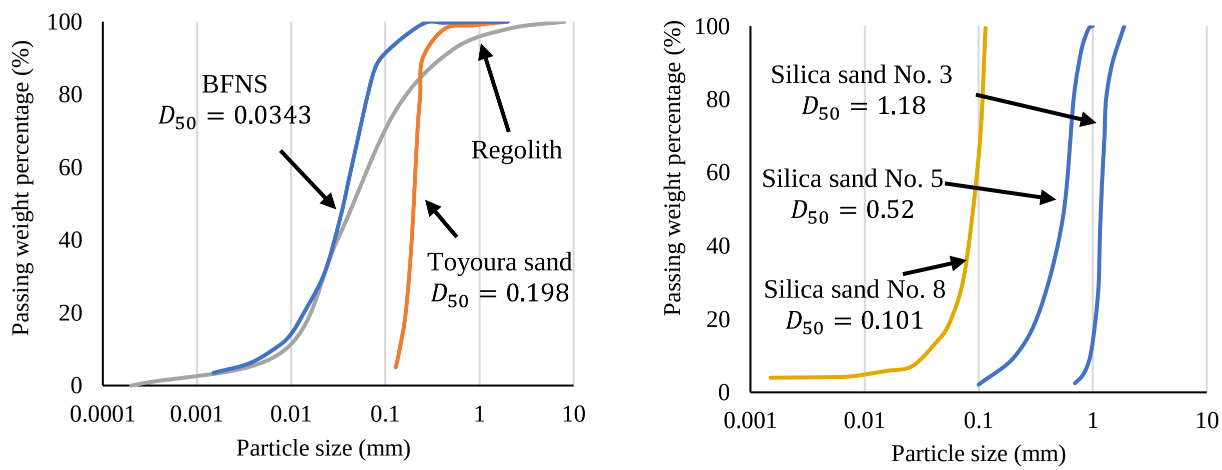

(a) Toyoura sand and BFNS, regolih

(b) Silica sand No.3 and No.5, No.8

Fig. 5. *Particle size distribution curves of the sand*

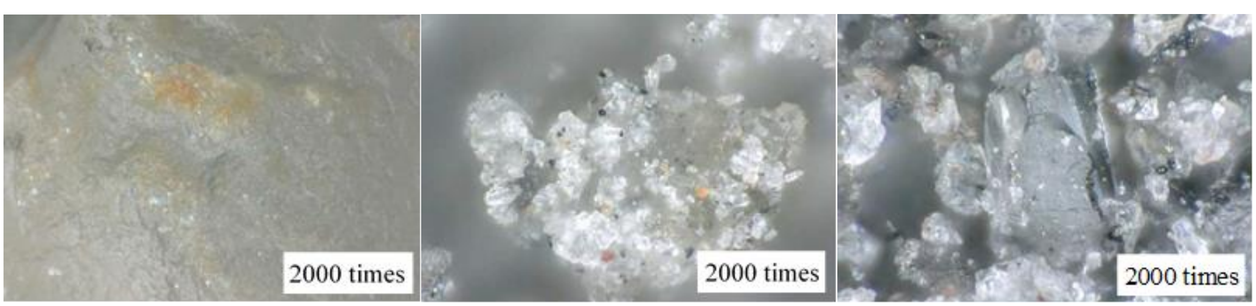

(a) Toyoura sand

(b) BFNS

(c) regolith simulant

Fig. 6. *Micrograph of the sand sample used in this experiment*

From Fig. 5, the similarity can be confirmed as the particle size distribution curves of regolith simulant and BFNS are closer than those of Toyoura sand. Also, from Fig. 6-(a), (b) and (c), the particle surfaces of regolith simulant and BFNS are observed to be more complex than Toyoura sand so regolith simulant and BFNS are confirmed the similarity.

A simple vane shear test was also conducted on these three sands. The depth of the blade of the simple vane shear tester used was 4.5 cm, and the blade was inserted until it was completely buried under the ground surface. Figure 7-(a) shows the results of vane shear tests of BFNS and Toyoura sand, and Fig. 7-(b) shows the results of vane shear tests of Silica sand No. 3, No. 5, and No. 8. Figure 7-(a) shows that the values of BFNS and regolith simulant are closer than those of Toyoura sand, which also confirms the similarity between the two. The fitted curves shown in Fig. 7, the result of $R^2 > 0.7$, which is generally said to show high correlation, is adopted, and the density obtained from this equation is used as the unit volume weight of sand in Eq. (1).

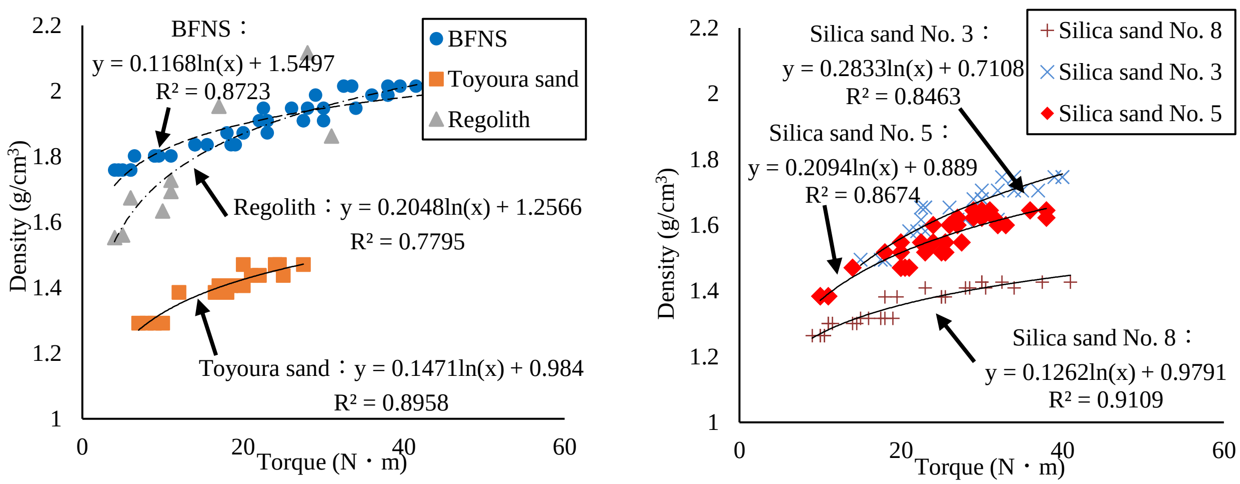

wh(a) Toyoura sand, BFNS, Regolith

(b) Silica sand No.3, No.5, No.8

Fig. 7. *the results of vane shear tests*

In summary, the similarity between the regolith simulant and BFNS was confirmed from the results of the particle size distribution curves, surface profile, and vane shear test. These sands were filled into a cylindrical container with a base diameter of 150 mm and packed about 360 mm high for the experiment. In addition, only the dry condition of the test ground is considered for the lunar surface, and the other factors such as low gravity and vacuum are not considered.

3. Experimental results and analysis

3.1 Comparison with vibration frequency

Figure-8 shows the relationship between the internal friction angle and the vibration frequency of the vibrating blade. The Fig. 8-(a) shows the results for BFNS and Toyoura sand, Fig. 8-(b) shows the results for silica sand No. 3, No. 5 and No. 8. From Fig. 8, it can be confirmed that the internal friction angle of the ground becomes smaller when the vibration frequency is increased, regardless of the sands. Also, it was confirmed that there was a difference in the decrease rate of the internal friction angle depending on the type of sand. In Fig. 8-(a), it can be confirmed that the internal friction angle of Toyoura sand is smaller than that of BFNS. This is probably due to the difference in particle shape and size. Since the surface of BFNS is angular, it is thought that the interlocking of the sand particles makes it difficult for the internal friction angle to decrease. Also, as the frequency of vibration increases, the rate of decreasing the internal friction angle tends to decrease. Hence, it can be inferred that there is an optimum frequency required for a decrease in the internal friction angle.

In Fig. 8-(b), it can be confirmed the tendency that the larger the particle size, the lower the internal friction angle even if when the sand was vibrating.

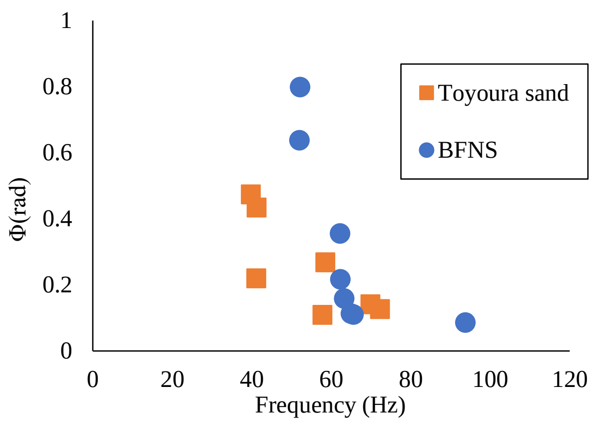

(a) Toyoura sand, BFNS, Regolith

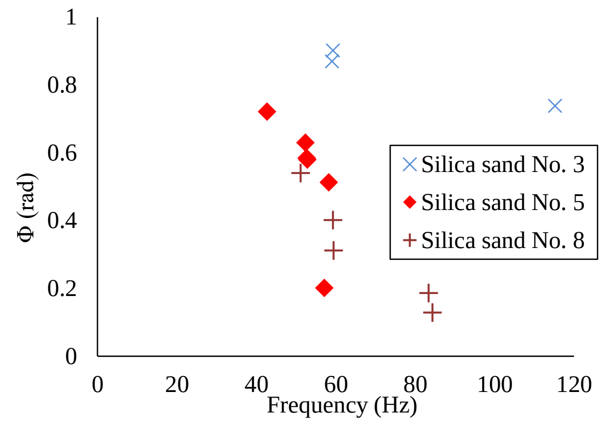

(b) Silica sand No.3, No.5, No.8

Fig. 8. *Comparison with the vibration frequency in this experiment*

3.2 Comparison with amplitude

Figure-9 shows the relationship between the internal friction angle and the amplitude of the vibrating blade. The Fig. 9-(a) shows the results for BFNS and Toyoura sand, Fig. 9-(b) shows the results for Silica sand No. 3, No. 5, and No. 8. From Fig. 9, it can be confirmed that the internal friction angle decreases as the amplitude increases, regardless of the sands. Also, it was confirmed that there was a difference in the decreasing rate of the internal friction angle depending on the type of sands. In Fig. 9-(a), as in the comparison of frequency (Fig. 8), the internal friction angle of Toyoura sand is smaller than that of BFNS. These are guessed due to differences in particle shape and size. Since the surface of BFNS is complex, it is thought that the interlocking of the sand particles led to the difficulty in decreasing the internal friction angle. Also, as the amplitude increases, the rate of the internal friction angle reduction tends to decrease. Therefore, we can guess the existence of an optimum required amplitude for the reduction of the internal friction angle. In Fig. 9-(b), the larger the particle size, the relatively larger the amplitude is required to decrease the internal friction angle.

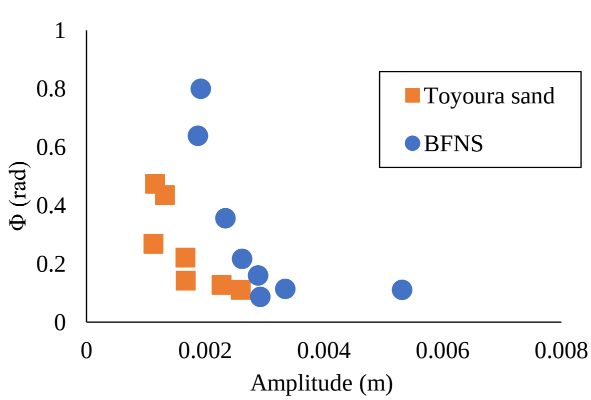

(a) Toyoura sand, BFNS, Regolith

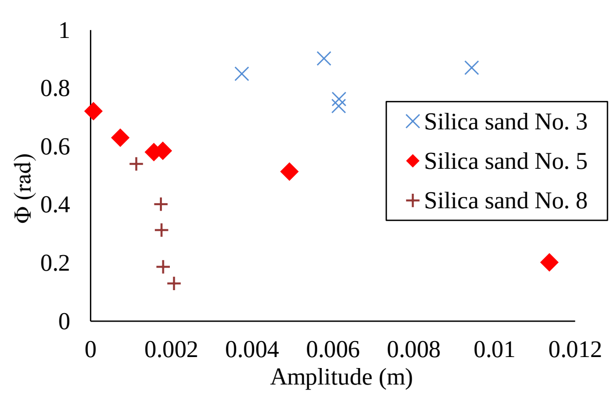

(b) Silica sand No.3, No.5, No.8

Fig. 9. *Comparison with amplitude in this experiment*

3.3 Comparison with vibration energy

In this experiment, amplitude was not constant when comparing frequencies, and frequency was not constant when comparing amplitudes because of the limitation of experimental device. Therefore, in order to consider both the frequency and amplitude, a comparison using the vibration energy was performed. Equation (2) shows the formula for calculating the vibration energy.

$$E = 2\pi^2 m f^2 A^2 \tag{2}$$

Here, E is the vibration energy, m is the mass of the vibrating blade, f is the frequency, and A is the amplitude. Figure-10 shows the relationship between internal friction angle and vibration energy using equation (2). Figure-10 (a) shows the results for BFNS and Toyoura sand, and (b) for Silica sand No. 3, Silica sand No. 5, and Silica sand No. 8. Figure-10 shows that the internal friction angle tends to decrease with the increase of vibration energy, regardless of the sands.

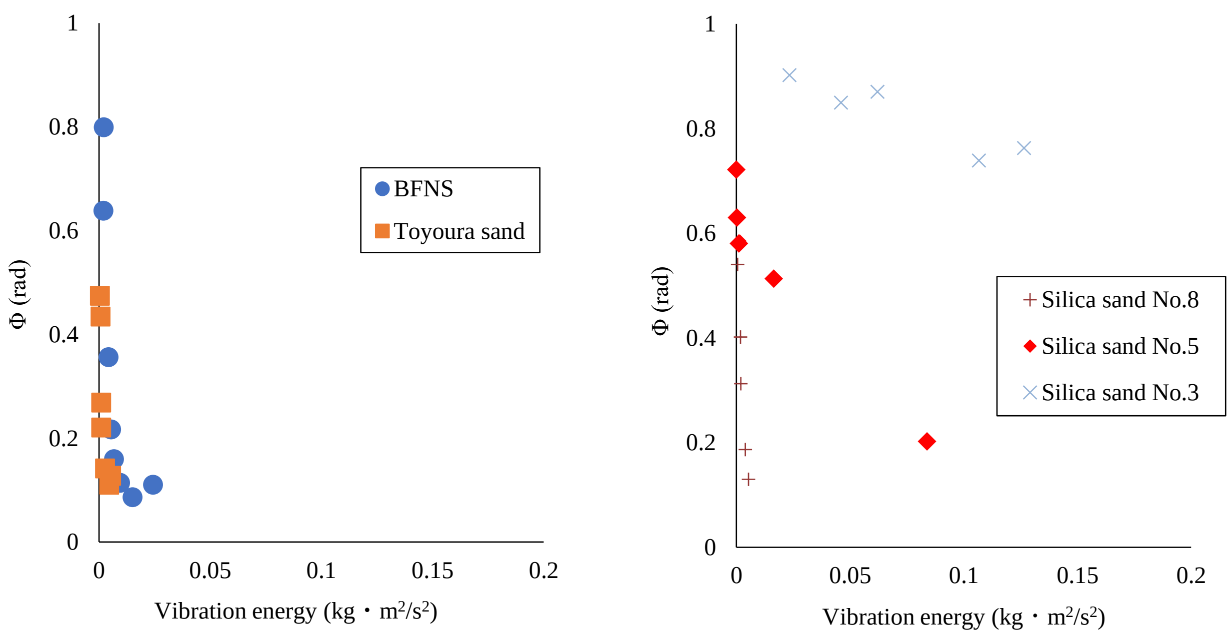

(a) Toyoura sand, BFNS, Regolith

(b) Silica sand No.3, No.5, No.8

Fig. 10. *Comparison with vibration energy in this experiment*

3.4 Effect of different particle size

As mentioned in section 3.2, the larger the particle size, the relatively larger amplitude of vibration is required to decrease the internal friction angle. Therefore, we focused on the amplitude of vibration and the average particle size of the sands to evaluate the reduction of the internal friction angle. Figure-11 shows a comparison of the relative resistance value and the measured amplitude divided by the average particle size of the sands. The figure is expressed in one-logarithm. In Fig.11, the relative resistance value means the ratio of the internal friction angle calculated by equation (1) using the amount of initial and final settlement.

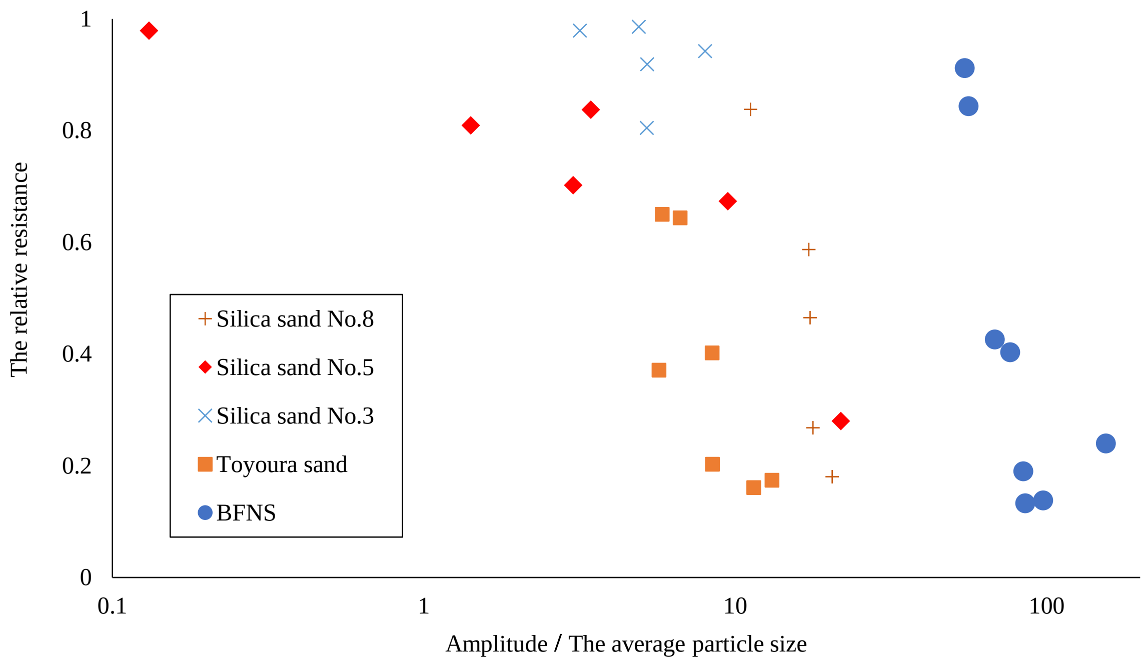

Fig. 11. *Relationship between amplitude/average particle size and The relative resistance*

In Fig.11, it can be confirmed that the internal friction angle tends to decrease rapidly when the amplitude/average particle size exceeds a certain value depending on the type of sand. The larger the particle size, the less the internal friction angle tends to decrease. This is possibly due to the effect of rotating when the sand particles scattered by vibration are rearranged. The reason why the internal friction angle tends to decrease with smaller particle size is thought to be that smaller particles require small movements to disengage the sand particles from each other, while larger particles require larger movements to disengage them (Takemura and Tateyama, 2012).

4. Conclusion and prospects

In this study, a basic study to demonstrate the effectiveness of vibration in lunar excavation, experiments were conducted to confirm the relationship between vibration and the angle of internal friction. The result of the experiment indicates the strength of the soil, and the effect of the frequency and amplitude of vibration on the angle of internal friction depending on the particle size and the several kinds of sands. The following are conclusions and prospects.

1) The internal friction angle showed a decreasing trend as frequent, amplitude, and vibration energy increased.

2) The tendency for the rate of decrease in the angle of internal friction to decrease with increasing vibration suggests the existence of an optimum vibration for the decrease in the angle of internal friction.

3) It was confirmed that there was a difference in decreasing rate in the angle of internal friction depending on the type of sand, such as BFNS and Toyoura sand in this experiment, and this is presumably due to the effect of particle shape and size. In particular, BFNS has many irregularities on the surface of the particles looks like lunar regolith, and it is thought that the interlocking of the irregularities makes it difficult for the internal friction angle to decrease.

4) Depending on the type of sand, the internal friction angle tends to decrease when the ratio of amplitude to average particle size exceeds a certain value. Therefore, it is expected that by adjusting the amplitude and frequency of vibration, it will be possible to estimate the vibration energy that can be used for efficient excavation while reducing the energy.

5) As a future work, based on the conclusions and considerations of 1) ~ 4), it is important to create a simple model and clarify theoretically the optimal vibration from the calculation.

References

EXEN, (Online). Available at: https://www.exen.co.jp/english.html (accessed 31 May 2021).

Hata, S., Muro, T., 1968. The Characteristics of the Moving Friction between a Plate and Dry Soil. Journal of the Society of Materials Science.Vol.17, No.174, 239-245. (in Japanese)

Takemura, Y., Tateyama, K., 2010. Optimization in some construction through effective use of oscillation. Proceedings of the 9th Asia – Pacific ISTVS Conference, 2010.